

# Development of a Ground Truth Localization System for Wheeled Mobile Robots in Indoor Environments based on Laser Range-finder for Low-cost Systems

Luis Piardi<sup>1</sup>, José Lima<sup>2,3</sup> and Paulo Costa<sup>3,4</sup>

<sup>1</sup>*Federal University of Technology, Paraná, Toledo, Brazil*

<sup>2</sup>*Research Centre in Digitalization and Intelligent Robotics (CeDRI), Instituto Politécnico de Bragança, Portugal*

<sup>3</sup>*INESC-TEC, Centre for Robotics in Industry and Intelligent Systems, Porto, Portugal*

<sup>4</sup>*Faculty of Engineering of University of Porto, Porto, Portugal*

**Keywords:** Robot Localization, Lidar, Ground Truth, Circular Fitting.

**Abstract:** The localization systems are becoming more and more required in the actual flexible manufacturing systems based on mobile robots. There are several approaches to localize a mobile robot such as laser scanners reflective beacons, image mapping, lightning based systems, Ultra-wideband time-of-flight trilateration, odometry and fusion sensor data algorithms. During the development phase of a localization methodology, it is necessary to evaluate the proposed system: it is used a ground truth system. Ground truth systems are precise (usually based on reflective beacons) but expensive. This paper presents a low-cost ground truth system based on a standard low-cost laser scanner that, coupled with the presented algorithm, allows to localize the robot in the field and thus evaluate other localization systems. Results of the precision of the developed system are presented and validates the approach.

## 1 INTRODUCTION

Nowadays, constant advances and several relevant applications have been emerging in the field of mobile agents in indoor environments. A great example is the autonomous mobile robots area. Thus, one of the main research areas employs efforts in the development of hardware and techniques such as Kalman and Particle filter to optimize the localization of these mobile agents, dealing with the complex minimization of errors and uncertainties due to noise.

Consequently, different methods are applied in the difficult task of locating mobile agents in internal environments, having different levels of precision and costs. The most common technologies are: Wi-Fi with an accuracy of 1-3 m (Zhong et al., 2016), bluetooth with an accuracy of 0.5 - 1 m (Rida et al., 2015) and Ultra Wide Band (UWB) (Lima and Costa, 2017) with an accuracy of 0.1 - 0.3 m. Methods based on data processing of cameras and Laser Range Finder (LRF) are also applied, however they have a higher price compared to the technologies previously mentioned.

The main contribution of this article is a proposal

of a low-cost ground-truth system, based on a popular LRF, for evaluation of one other localization system under development. It can be used in one indoor mobile robot localization system and it will localize one object with a circular geometric shape within its line of sight. This object is easily coupled to the mobile agent.

An outline of this paper is as follows. In Section 2 the state of the art of the main applications with LRF is presented. In Section 3 the methodology with the description of the sensor and the object is addressed, besides presenting the calculations involved in the proposed approach. Experimental results are presented in Section 4 and Section 5 concludes the paper.

## 2 RELATED WORK

Currently the laser-based scanner technology has provided the ability to develop applications for precise and fast non-contact measurement in a wide range of applications.

The laser range finder is applied for 2D mapping

(i.e., a laser that scans in one plane) and 3D mapping (i.e., a laser that scans and “nods” thus producing a range image of an area) (Okubo et al., 2009). In the present work it will be focused on the application of laser in 2D scan once it is computationally more efficient in the process of tracking an object.

In the last decade the LRF with 2D scanning was applied in several activities in mobile robotics, such as detecting and avoiding collision with obstacles. In (Xu et al., 2006), was proposed a method for obstacle detection based on stochastic density of scan points using a robot equipped with a laser scanner in structural or semi/non-structural environment. Another example is the paper (Zeng and Weng, 2007) where a mobile humanoid robot is equipped with a 2D laser scanner to detect and avoid static and dynamic obstacles through on-line real-time incremental learning.

The 2D Laser Range Finder is also widely applied for the construction of maps in a single slice of the plan (Nepali et al., 2015; Olson, 2015). In (Nepali et al., 2015) the LRF data are used together with segmentation algorithm methods, Split and Marge algorithm and best algorithm for reconstruct floor plans with centimeter precision. However, these techniques accumulate errors and have a considerable computational cost (Hess et al., 2016).

In this same context, the LRF has been amply used in simultaneous localization and mapping (SLAM) problem. SLAM addresses the problem of robot navigation in an unknown environment (Siciliano and Khatib, 2008; Santos et al., 2013). In (Sobreira et al., 2015) was used a security laser presented on most of industrial AGVs for traveling in the unknown environment, while generating the map and at the same time it wishes to localize itself using its map.

More related to this work is the use of an external and fixed LRF to perform the tracking of cylindrical objects attached to moving devices such as mobile robot. Teixidó et al. (Teixidó et al., 2012) combined the information obtained from an external fixed LRF with algorithm for outlier avoidance and a least-squares circular fitting to detect cylindrical targets attached to moving devices (Teixidó et al., 2012).

Given the wide range of applications of the LRF and the wide acceptance of academia and industry in its use, the present work will be composed by a laser scanner to perform mobile robot tracking in internal environments, i.e. a ground truth to validate low cost localization systems based on other emerging technologies such as Ultra Wide Band.

### 3 METHODOLOGY

This section, will present the methods and materials used in this work for the development of the ground truth system to track a circular object.

#### 3.1 Hokuyo Sensor Description

This application uses the Hokuyo URG-04LX sensor (Kawata, 2006) to evaluate others low cost systems for the tracking of mobile robots (Figure 1). It has a good resolution and specifications compared to the same equipment in its price range around one thousand Euros.



Figure 1: URG-04LX laser sensor manufactured by Hokuyo.

The LRF scans the area around it to determine the distance of closest objects, providing a two-dimensional map of the environment with high accuracy. The principle of operation is based on the emission of a sinusoidally modulated laser beam. A rotating mirror changes the beams direction, then the laser hits the surface of an object and is reflected. The direction of the reflected light is changed again by a rotating mirror, and captured by the photo diode. The phases of the emitted and received light are compared and the distance between the sensor and the object is calculated (Lima et al., 2013). Figure 2 illustrates the activity of the LRF.

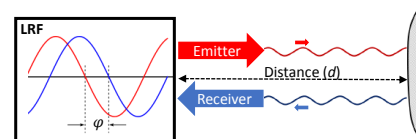


Figure 2: Measurement of the phase between the waves emitted and received by the LRF.

Since the emitted and reflected waves have the same frequency  $f$  as shown in Figure 2, it is possible to determine the distance between the sensor and the surface from the equation 1, where  $d$  is the distance

between the LRF and a surface.

$$d = \frac{c \cdot \varphi}{4 \cdot \pi \cdot f} \quad (1)$$

The variable  $\varphi$  is the phase difference between the waves emitted and received in radians. The constant  $c$  indicates the wave propagation velocity in the environment.

The relevant specifications obtained from the manufacturer for the Hokuyo URG-04LX can be checked in Table 1 (Hokuyou, 2018).

Table 1: Sensor LRF URG-04LX specifications.

Specifications	URG-04LX	Unit
Measuring Area	20 to 5,600	mm
Accuracy	60 to 1,000 : $\pm 30$ 1,000 to 5,600 $\pm 3\%$	mm
Ang. Resolution	$0.36^\circ$ ( $360^\circ/1024$ )	deg
Scanning Time	100	ms
Consumption	2.5	W
Wight	0.16	Kg

The sensor takes only 100ms for a 240 degrees scan. During each scan, the Hokuyo URG-04-LX laser range finder returns 683 distance measurements via its USB interface (Kawata, 2006).

### 3.2 Ground Truth Range

Figure 3 shows the range of the ground truth, i.e. the measurement area of the LRF. The LRF is installed in the origin of the frame that represents tracking environment. The laser is fixed in position (0, 0) of the 2D plane where a polar mapping with a radius of 5.6 m and an angle comprised of from -120 degrees to +120 degrees.

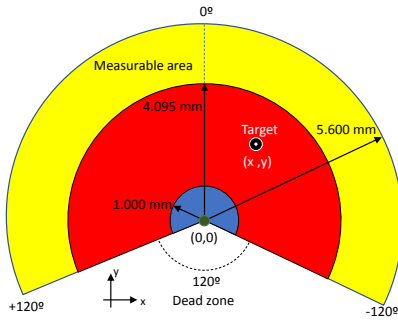


Figure 3: Ground truth operation and tracking region.

The blue region represents the area with a precision of 30 mm of localization. Red region delimits the area where the sensor's operating mode provides 12 bits of distance and angle data. This region is widely used by the academic community, for example (Lima

et al., 2013; Okubo et al., 2009). The area in yellow includes the maximum region of measuring stipulated by the manufacturer and the sensor operating mode provide 18 bits of data (Kawata, 2006).

### 3.3 Object Description

The object targets used in this paper was a drum lampshade with a diameter of 0.25 m. Within the measurable area, LRF locates a circle with the same diameter of target and returns the position  $(x_c, y_c)$  of its center point as showed in Figure 4.

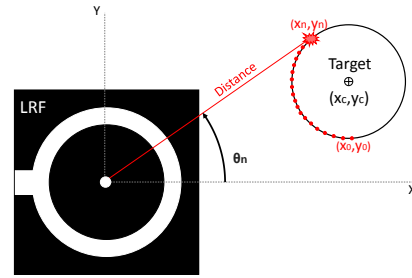


Figure 4: Fixed laser scanner to detect cylindrical target and return the center position  $(x_c, y_c)$ .

This target was easily fixed to the mobile robot (it can also be fixed to other mobile devices) and it is possible to estimate its position and trajectory. In the case of the mobile robot with differential drive, the center of the object must be aligned with the center point of the traction wheel axis, i.e., the origin of the axis of rotation, avoiding measurement errors. Figure 5a presents a robot that is incapable of being traceable by this approach. Figure 5b shows the robot equipped with the object, which makes it traceable.

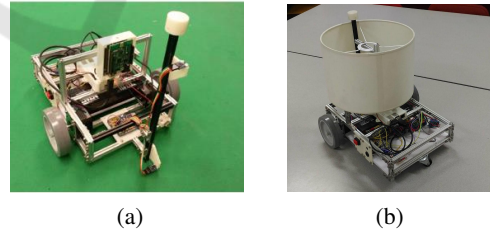


Figure 5: Cylindrical target: (a) Mobile robot without target. (b) Mobile robot with target used.

### 3.4 Circular Fitting Calculation

The data from the LRF is in the polar form coordinate i.e. distance and angle. But the tracking is carried out in Cartesian coordinate. So the scan data in polar coordinate needs to be converted into Cartesian coordinate using the sine trigonometry identity, as show in the following equations:

$$x_i = d_i * \cos(\theta_i) \quad (2)$$

$$y_i = d_i * \sin(\theta_i) \quad (3)$$

Given a finite set of points representing the edge of the target in  $\mathbb{R}^2$ ,  $\{(x_i, y_i) | 0 \leq i < n\}$ , it is necessary to find the circle that (in a least-squares sense) fits the points. First of all, it finds the mean values of x and y, as presented in next equations.

$$\bar{x} = \frac{1}{n} \sum_i x_i \quad \text{and} \quad \bar{y} = \frac{1}{n} \sum_i y_i \quad (4)$$

The problem is solved firstly in the coordinates  $(u, v)$  where  $u_i = x_i - \bar{x}$  and  $v_i = y_i - \bar{y}$ . Then, transforms it back to  $(x, y)$  coordinates.

Let the circumference has the center at  $(u_c, v_c)$  and radius R. The algorithm minimizes

$$S = \sum_i (g(u_i, v_i))^2 \quad (5)$$

where

$$g(u, v) = (u - u_c)^2 + (v - v_c)^2 - \alpha \quad (6)$$

and

$$\alpha = R^2 \quad (7)$$

To minimize S, the procedure is to differentiate  $S(\alpha, u_c, v_c)$ .

$$\frac{\partial S}{\partial \alpha} = 2 \sum_i g(u_i, v_i) \frac{\partial g}{\partial \alpha}(u_i, v_i) = -2 \sum_i g(u_i, v_i) \quad (8)$$

Thus, if the radius variation is zero, i.e.  $\partial S / \partial \alpha = 0$  then:

$$\sum_i g(u_i, v_i) = 0 \quad (9)$$

Continuing, the differentiation of S with respect to  $u_c$  results in:

$$\frac{\partial S}{\partial u_c} = 2 \sum_i g(u_i, v_i) \frac{\partial g}{\partial u_c}(u_i, v_i) \quad (10)$$

$$= 2 \sum_i g(u_i, v_i) 2(u_i - u_c)(-1) \quad (11)$$

$$= -4 \sum_i (u_i - u_c) g(u_i, v_i) \quad (12)$$

$$= -4 \sum_i u_i g(u_i, v_i) + 4u_c \underbrace{\sum_i g(u_i, v_i)}_{=0 \text{ by Eq. 9}} \quad (13)$$

Therefore, considering the radius of the constant target (Eq. 9) and fixed center point ( $\partial S / \partial u_c = 0$ ) the following equation is obtained:

$$\sum_i u_i g(u_i, v_i) = 0 \quad (14)$$

Similarly, requiring  $\partial S / \partial u_c = 0$  gives

$$\sum_i u_i g(u_i, v_i) = 0 \quad (15)$$

Expanding Equation 14 gives:

$$\sum_i u_i [u_i^2 + -2u_i u_c + u_c^2 + v_i^2 - 2v_i v_c + v_c - \alpha] = 0 \quad (16)$$

Defining  $S_u = \sum_i u_i$ ,  $S_{uu} = \sum_i u_i^2$  and so on, it is possible to rewrite the equation (16) as:

$$S_{uu} - 2u_c S_{uu} + u_c^2 S_u + S_{uvv} - 2v_c S_{uv} + v_c^2 S_u - \alpha S_u = 0 \quad (17)$$

Since  $S_u = 0$ , this simplifies to

$$u_c S_{uu} + v_c S_{uv} = \frac{1}{2} (S_{uuu} + S_{uvv}) \quad (18)$$

In a similar way, expanding equation 15 and using  $S_v = 0$  gives:

$$u_c S_{uv} + v_c S_{uv} = \frac{1}{2} (S_{vvv} + S_{vuu}) \quad (19)$$

Solving equation 18 and 19 simultaneously gives  $(u_c, v_c)$ . Then, going back to  $(x, y)$  coordinates, the real center point of the target  $(x_c, y_c)$  is obtained by the follow relation:

$$(x_c, y_c) = (u_c, v_c) + (\bar{x}, \bar{y}) \quad (20)$$

To find the radius R, equation 9 should be expanded:

$$\sum_i [u_i^2 - 2u_i u_c + u_c^2 + v_i^2 - 2v_i v_c + v_c^2 - \alpha] = 0 \quad (21)$$

Using  $S_u = S_v = 0$  again, it can be obtained  $R^2$  using equation below:

$$n(u_c^2 + v_c^2 - \alpha) + S_{uu} + S_{vv} = 0 \quad (22)$$

$$R^2 = \alpha = u_c^2 + v_c^2 + \frac{S_{uu} + S_{vv}}{n} \quad (23)$$

### 3.5 Laser Scan Application Developed

An application was developed in the Lazarus environment to operate the LRF and decode the received data. It is responsible for tracking the circumference, as well as being an user interface that allows the definition of parameters such as the region of interest of the sensor scanning, the value of the radius and its tolerance as shown in Figure 6.

Communication between the sensor and the application is done through a communication protocol called SCIP2.0, developed by the research group of the Intelligent Robot Laboratory of the University of Tsukuba. The communication rate is 9 Mbps through an USB port (Kawata, 2006). This application is also capable of performing wireless communication with another device through a UDP/IP protocol.

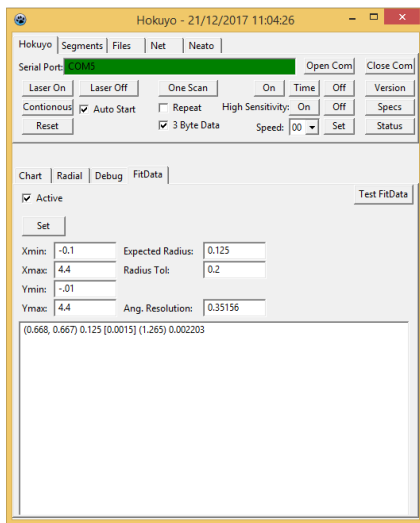


Figure 6: Application interface developed to operate the LRF.

## 4 RESULTS

The results of this paper will be divided into two parts. The first part, a structure with a robotic manipulator was adopted to evaluate the accuracy of the proposed system. In the second part, a mobile robot was used to evaluate five critical points in an area of  $16 \text{ m}^2$ . All data presented in this section refers to the center point  $(x_c, y_c)$  of the object that was subjected to the tracking.

### 4.1 Target Attached to a Robotic Manipulator

In order to obtain an accuracy analysis of the ground truth, the cylindrical object described above was attached to the tool of ABB IRB 1400 robotic manipulator, which has a linear path repeatability of at maximum  $0.25 \text{ mm}$  according to the manufacturer (ABB, 2003). The structure can be seen in Figure 7. The center of the sensor represents the point  $(0,0)$  of the 2D plane scanned by the device, indicated by the red axes.

The robotic manipulator was positioned at 100 different points/locations  $(x, y)$  forming an array of  $[5 \ 20]$  (See Figure 8). It is worth mentioning that the size of the area respects the reach and limitations of the manipulator. An algorithm was developed to control the manipulator by equally spacing the points in the X direction by  $0.05 \text{ m}$  and in the Y direction by  $0.1 \text{ m}$ . At each position of this matrix 200 samples were obtained. At all locations in the matrix, the error lies within a circle of  $0.01 \text{ m}$  in diameter (red Circles



Figure 7: Structure adopted to perform ground truth precision tests.

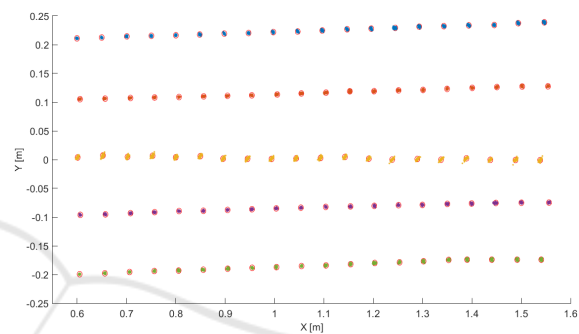


Figure 8: Measurements obtained at 100 different locations of the 2D plane using the ABB IRB 1400 robot manipulator.

of Figure 8).

Another test was performed with this same structure of the robotic manipulator. A linear trajectory with a constant velocity of  $0.25 \text{ m/s}$  was made by performing a rectangular circuit. The points  $(x; y)$  visited by the tool of manipulator were respectively  $(0.6; 0.2)$ ,  $(1.1; 0.2)$ ,  $(1.1; -0.2)$ ,  $(0.6; -0.2)$  and finally  $(0.6; 0.2)$ . Figure 9 shows the path traveled and the points sampled by the ground truth.

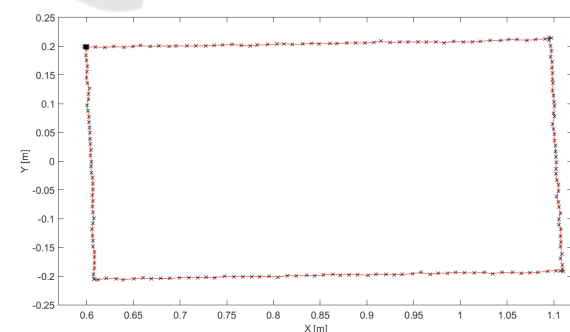


Figure 9: Linear path performed by robotic manipulator and cylindrical object tracked by ground truth system.

### 4.2 Target Attached to a Mobile Robot

For this subsection, an area of  $4 \times 4 \text{ m}$  was organized to perform the tracking in five different positions (A,

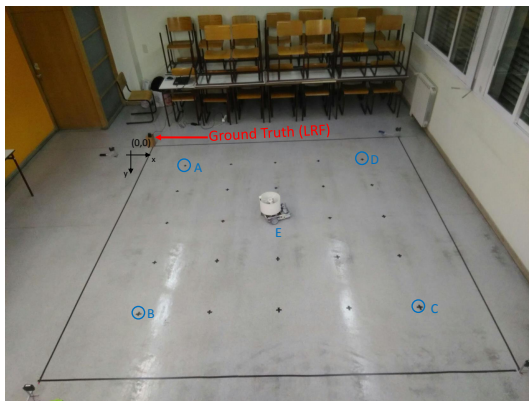


Figure 10: Structure adopted to perform ground truth with mobile robot.

B, C, D, E) using a mobile robot with the cylindrical object (see Figure 10).

This area totaling  $16\text{ m}^2$  is contained inside the range of the LRF as shown the illustration in Figure 11.

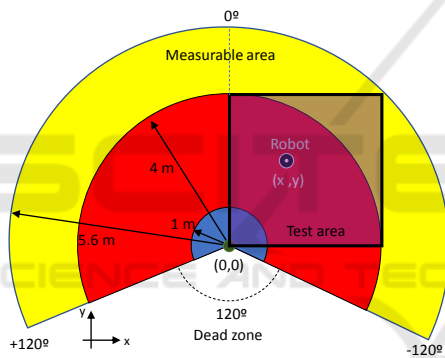


Figure 11: Testing area respecting the specifications of the LRF.

Table 2 shows the position of each point that the mobile robot was positioned. 400 samples were taken for each position.

Table 2: Positions used for data acquisition.

Position	Position X [m]	Position Y [m]
A	0.67	0.67
B	0.67	3.33
C	3.33	3.33
D	3.33	0.67
E	2.01	2.01

Table 3 shows the mean and standard deviation of the 400 samples obtained with the ground truth for each point by measuring the proposed system's dispersion.

The following Figures show the frequency distribution (histogram) for each of the points in X and Y

Table 3: Mean and standard deviation of the error obtained with the ground truth.

Pos	Mean X	Mean Y	Std X	Std Y
A	0.0001	-0.0028	0.0013	0.0012
B	-0.0024	0.0004	0.0024	0.0024
C	-0.0117	0.0050	0.0043	0.0042
D	0.0083	-0.0013	0.0017	0.0024
E	0.0189	0.0348	0.0016	0.0017

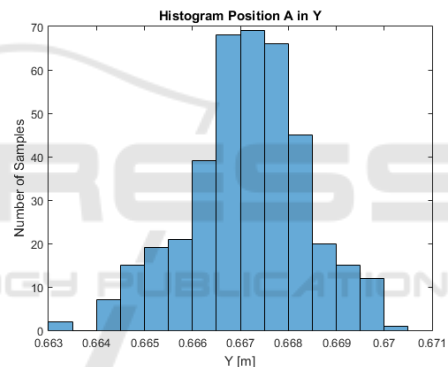
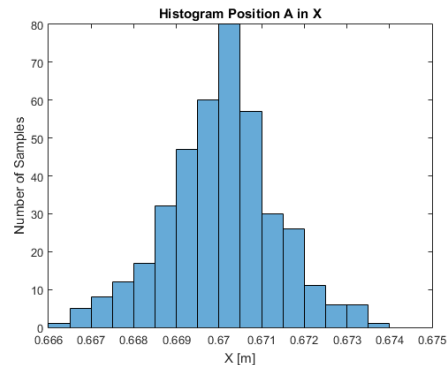


Figure 12: Histogram of position A in the X and Y directions.

component. It is possible to notice that most of the obtained data have a normal distribution.

The developed system presents an absolute average error of 8 mm in X axis and 9 mm in Y axis.

## 5 CONCLUSIONS

This paper proposed the use of an LRF to locate and detect an object in the form of a circle in a 2D plane, in order to validate (as ground truth) the low cost location systems for mobile robots. The used sensor was the URG-04LX manufactured by Hokuyo and the target was a cylinder with a diameter of 0.25 m. To test the system performance two scenarios were used: one with the target mounted on an industrial manipulator and other with the target mounted on a mobile robot. In both cases, low noise was observed in the

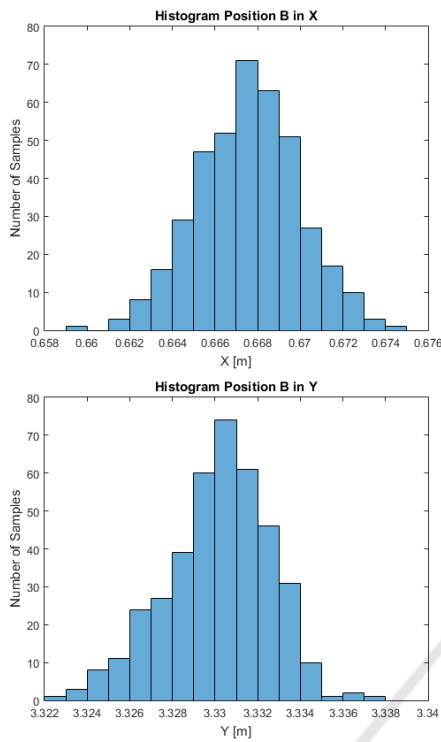


Figure 13: Histogram of position B in the X and Y directions.

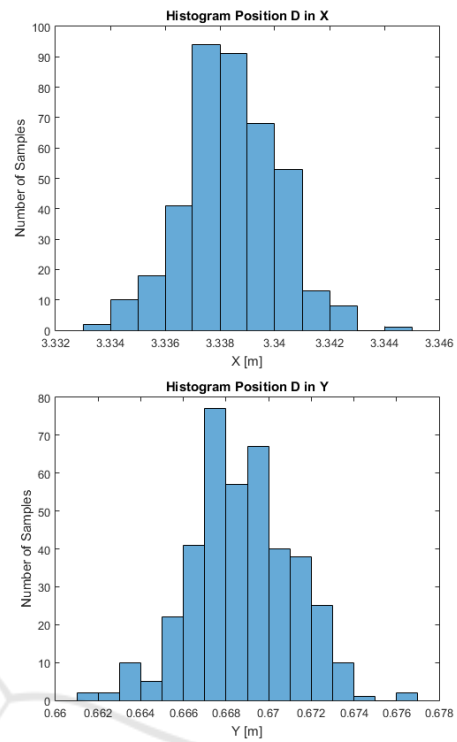


Figure 15: Histogram of position D in the X and Y directions.

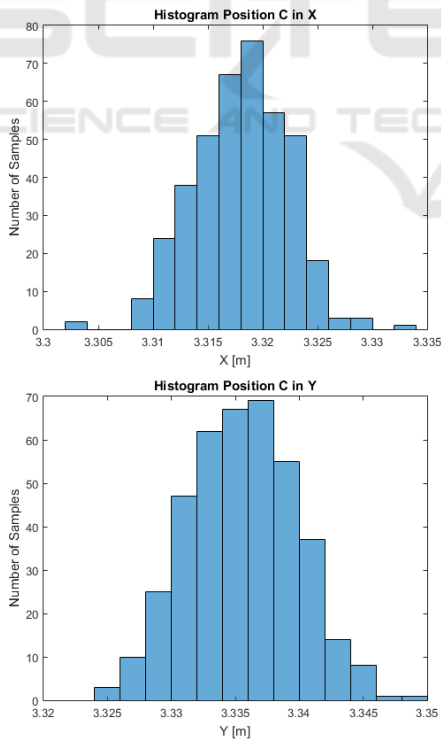


Figure 14: Histogram of position C in the X and Y directions.

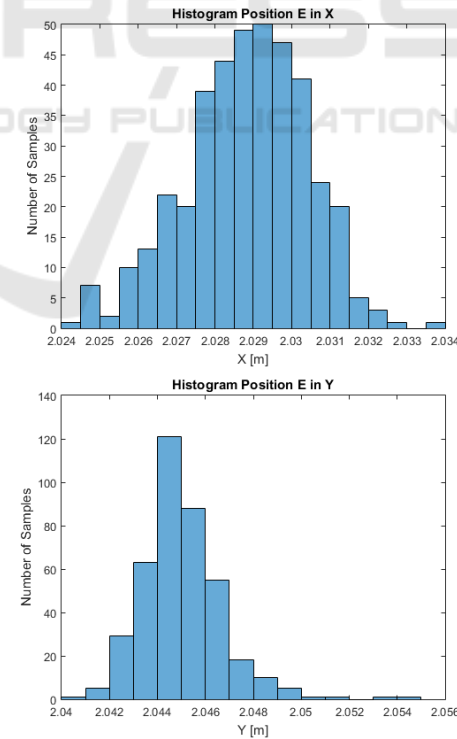


Figure 16: Histogram of position E in the X and Y directions.

localization of the target even with a mis-calibration between the manipulator and the sensor frames. The results validated the proposed methodology for a low-cost ground-truth system to be used in mobile robotic applications.

Finally, as future work is intended to develop a standardized bench to optimize the alignment of the sensor and apply the ground truth in a low cost localization application and the development of a ROS node enhancing the cooperation among other researchers community.

## ACKNOWLEDGEMENTS

This work is financed by the ERDF European Regional Development Fund through the Operational Programme for Competitiveness and Internationalisation - COMPETE 2020 Programme within project POCI-01-0145-FEDER-006961, and by National Funds through the Portuguese funding agency, FCT -Fundação para a Ciência e a Tecnologia (Portuguese Foundation for Science and Technology), within project SAICTPAC/0034/2015- POCI-01- 0145-FEDER-016418 and as part of project UID/EEA/50014/2013.

## REFERENCES

- ABB, R. (2003). Product manual irb 140. *ABB Robotics Products AB publication*, (M2000):7564–1.
- Hess, W., Kohler, D., Rapp, H., and Andor, D. (2016). Real-time loop closure in 2d lidar slam. In *Robotics and Automation (ICRA), 2016 IEEE International Conference on*, pages 1271–1278. IEEE.
- Hokuyou (2018). Urg-04lx. Online; accessed 29/01/2018.
- Kawata, H. (2006). Urg series communication protocol specification scip-version2. 0. *Drawing No. C-42-03320B, Oct.*
- Lima, J. and Costa, P. (2017). Ultra-wideband time of flight based localization system and odometry fusion for a scanning 3 dof magnetic field autonomous robot. In *Iberian Robotics conference*, pages 879–890. Springer.
- Lima, J., Gonçalves, J., Costa, P. J., and Moreira, A. P. (2013). Modeling and simulation of a laser scanner sensor: an industrial application case study. pages 245–258.
- Nepali, M. R., Yadav, N., Dev, U., Mishra, S., and Shrestha, S. L. (2015). A strategic methodology for 2d map building in an indoor environment. In *Next Generation Computing Technologies (NGCT), 2015 1st International Conference on*, pages 797–803. IEEE.
- Okubo, Y., Ye, C., and Borenstein, J. (2009). Characterization of the hokuyo urg-04lx laser rangefinder for mobile robot obstacle negotiation. In *Unmanned Systems Technology XI*, volume 7332, page 733212. International Society for Optics and Photonics.
- Olson, E. (2015). M3rsm: Many-to-many multi-resolution scan matching. In *Robotics and Automation (ICRA), 2015 IEEE International Conference on*, pages 5815–5821. IEEE.
- Rida, M. E., Liu, F., Jadi, Y., Algawhari, A. A. A., and Askourih, A. (2015). Indoor location position based on bluetooth signal strength. In *Information Science and Control Engineering (ICISCE), 2015 2nd International Conference on*, pages 769–773. IEEE.
- Santos, J. M., Portugal, D., and Rocha, R. P. (2013). An evaluation of 2d slam techniques available in robot operating system. In *Safety, Security, and Rescue Robotics (SSRR), 2013 IEEE International Symposium on*, pages 1–6. IEEE.
- Siciliano, B. and Khatib, O. (2008). *Springer handbook of robotics*. Springer Science & Business Media.
- Sobreira, H., Moreira, A. P., Costa, P. G., and Lima, J. (2015). Robust mobile robot localization based on security laser scanner. In *Autonomous Robot Systems and Competitions (ICARSC), 2015 IEEE International Conference on*, pages 162–167. IEEE.
- Teixidó, M., Pallejà, T., Font, D., Tresanchez, M., Moreno, J., and Palacín, J. (2012). Two-dimensional radial laser scanning for circular marker detection and external mobile robot tracking. *Sensors*, 12(12):16482–16497.
- Xu, Z., Zhuang, Y., and Chen, H. (2006). Obstacle detection and road following using laser scanner. In *Intelligent Control and Automation, 2006. WCICA 2006. The Sixth World Congress on*, volume 2, pages 8630–8634. IEEE.
- Zeng, S. and Weng, J. (2007). Online-learning and attention-based approach to obstacle avoidance using a range finder. *Journal of Intelligent and Robotic Systems*, 50(3):219–239.
- Zhong, Y., Wu, F., Zhang, J., and Dong, B. (2016). Wifi indoor localization based on k-means. In *Audio, Language and Image Processing (ICALIP), 2016 International Conference on*, pages 663–667. IEEE.